

<Supporting Information>

Narcissistic self-sorting vs. statistic ligand shuffling within a series of phenothiazine-based coordination cages

Contents

1. Crystal Structure Analysis	2
2. ¹ H NMR and ESI-MS spectra of the mixing experiments	5
2.1.1 Mixture of ligands L ¹ and L ² and cages [Pd ₄ L ¹ ₈] and [Pd ₄ L ² ₈]	5
2.1.2 Mixture of ligands L ² and L ³ and cages [Pd ₄ L ² ₈] and [Pd ₄ L ³ ₈]	6
2.1.3 Mixture of ligands L ² and L ⁴ and cages [Pd ₄ L ² ₈] and [Pd ₂ L ⁴ ₄]	7
2.1.4 Mixture of ligands L ³ and L ⁴ and cages [Pd ₄ L ³ ₈] and [Pd ₂ L ⁴ ₄]	8
2.1.5 Mixture of cages [Pd ₄ L ¹ ₈] and [Pd ₄ L ³ ₈] and 2-Picoline	9
2.1.6 Temporal evolution of the heated samples of the mixture of ligands L ¹ and L ³ and cages [Pd ₄ L ¹ ₈] and [Pd ₄ L ³ ₈]	10

1. Crystal Structure Analysis

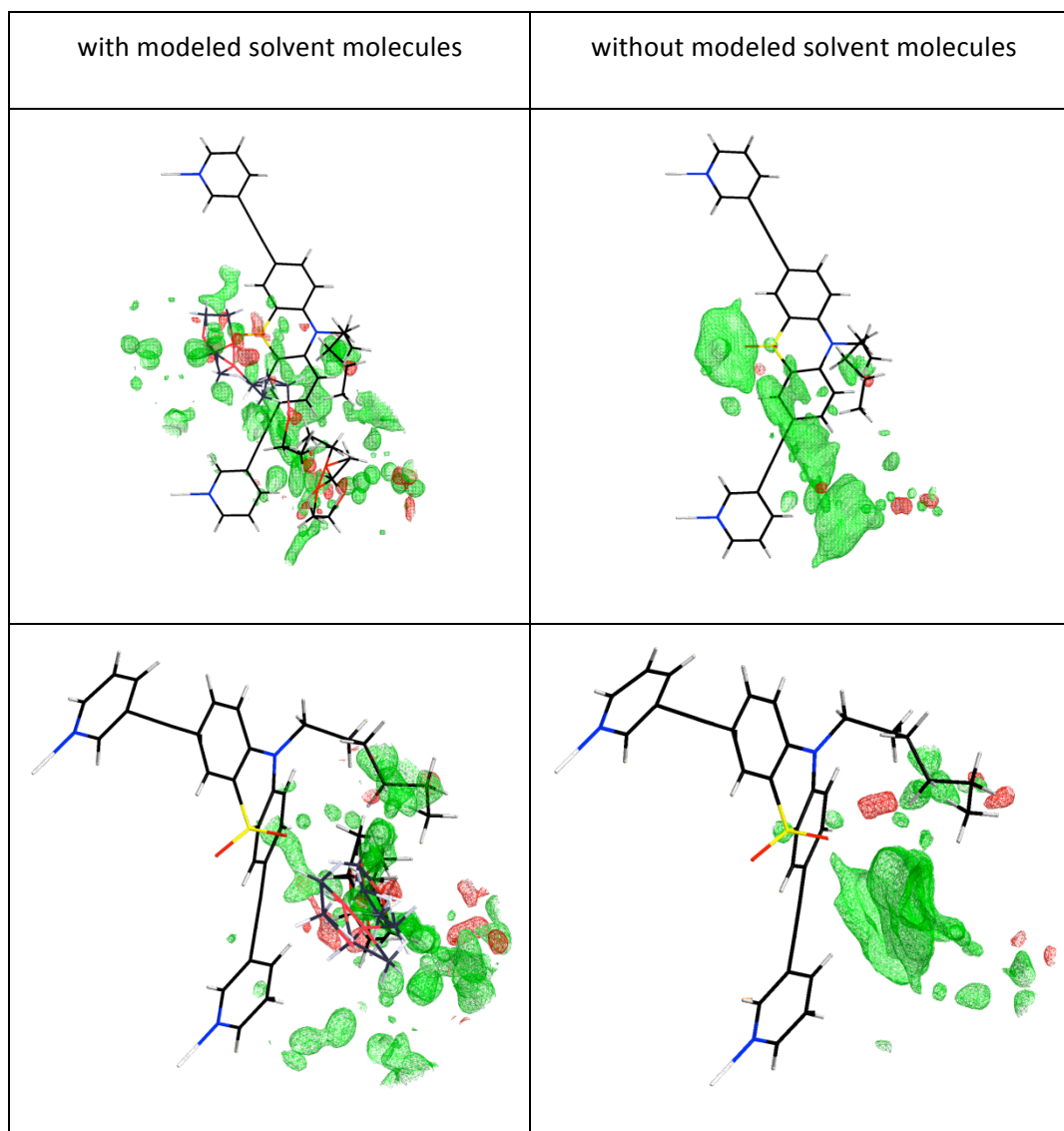


Fig. SI-1 Exemplification of the solvent accessible crystal voids.

The pictures only show the residual electron density in the solvent channels of one asymmetric unit, the rest of the density and the BF_4^- ions are omitted for clarity. Due to the low resolution of the data, it was not possible to adequately model the lattice solvent into these voids and get a stable refinement. In order to extinguish the influence of the electron density present in the voids, the SQUEEZE routine of the PLATON program package was used.¹

Table SI-1 Comparison of final model quality indicators.

	without solvent	with solvent	squeeze
R1	0.1158	0.0970	0.0797
wR2	0.3977	0.3804	0.3011
GooF*	1.360	1.612	1.010

*restrained GooF for all data

In conclusion, the utilization of the SQUEEZE routine led to a significant improvement of the model quality of the cage and its counterions. Check-cif data can be found in the reference section.²

Comparison of Crystal Packing of $[\text{Pd}_4\text{L}^1_8]$, $[\text{Pd}_4\text{L}^2_8]$ and $[\text{Pd}_4\text{L}^3_8]$

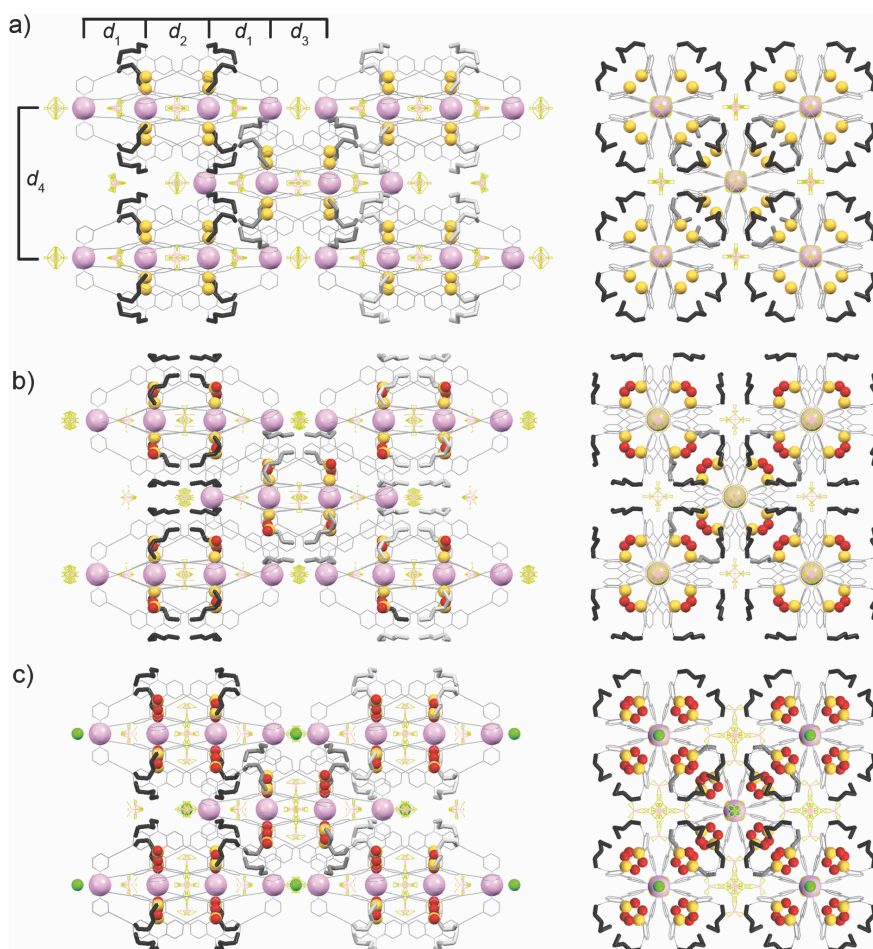


Fig. SI-2 Side view (left) and view along (right) the Pd_n -axis of nine selected cages extracted from the X-ray crystal packing of (a) $[\text{Pd}_4\text{L}^1_8]$, (b) $[\text{Pd}_4\text{L}^2_8]$ and (c) $[\text{Pd}_4\text{L}^3_8]$ (only anions positioned on the Pd_n -axis are shown, other anions and solvent molecules were omitted for clarity. C: grey, N: blue, O: red, S: yellow, B: brown, F: light green, Cl: dark green, Pd: purple). The hexyl residues are highlighted in the colours black, grey and silver to indicate different planes in the packing.

Table SI-2 Parameters of the cage structures and packing extracted from the crystal structures.

	[Pd ₄ L ¹ ₈]	[Pd ₄ L ² ₈]	[Pd ₄ L ³ ₈]
d_1 (Pd _{outer} -Pd _{inner})	8.77 Å	8.16 Å	8.40 Å
d_2 (Pd _{inner} -Pd _{inner})	8.85 Å	8.63 Å	8.47 Å
d_3 (Pd _{outer} -Pd _{outer})	7.88 Å	7.77 Å	6.54 Å
d_4 (Pd _{Cage} -Pd _{Cage})	21.12 Å	21.96 Å	21.99 Å

The Pd-Pd distances for a BF₄⁻ enclosed between two Pd(pyridine)₄ planes is at least 7.77 Å. The minimum Pd-Pd distance for a Cl⁻ is considerably smaller. It was found to be 6.54 Å for the Pd_{outer}-Pd_{outer} distance in the [Pd₄L³₈] double-cage (for comparison: the distance between two inner Palladium cations enclosing a chloride anion of a previously reported double-cage based on the suberone backbone was found to be 6.26 Å).³

2. ^1H NMR and ESI-MS spectra of the mixing experiments

2.1.1 Mixture of ligands L^1 and L^2 and cages $[\text{Pd}_4\text{L}^1_8]$ and $[\text{Pd}_4\text{L}^2_8]$

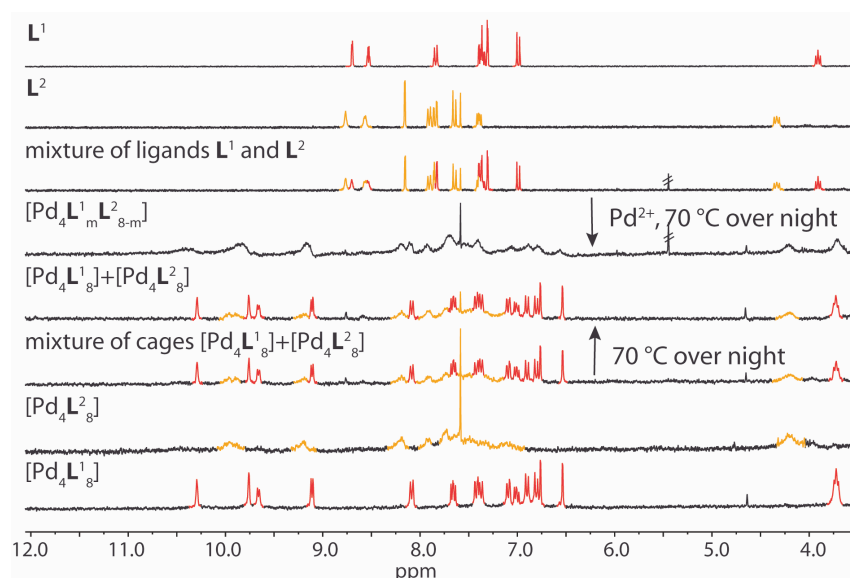


Fig. SI-3 ^1H NMR spectra (300 MHz, 298 K, CD_3CN) of a binary system containing two different long ligands L^1 + L^2 (250 μL of a 2.8 mM solution for each ligand). The outcome of the self-assembly gives mixed cages $[\text{Pd}_4\text{L}^1_m\text{L}^2_{8-m}]$, showing a statistical ligand distribution when the ligands are mixed prior to the addition of palladium and heating at 70 $^\circ\text{C}$ over night. In contrast, combining two preassembled double-cages $[\text{Pd}_4\text{L}^1_8]$ + $[\text{Pd}_4\text{L}^2_8]$ (250 μL of a 0.35 mM solution for each cage) leads to a mixture of coexisting homogeneous structures between which ligand exchange is tremendously slowed down.

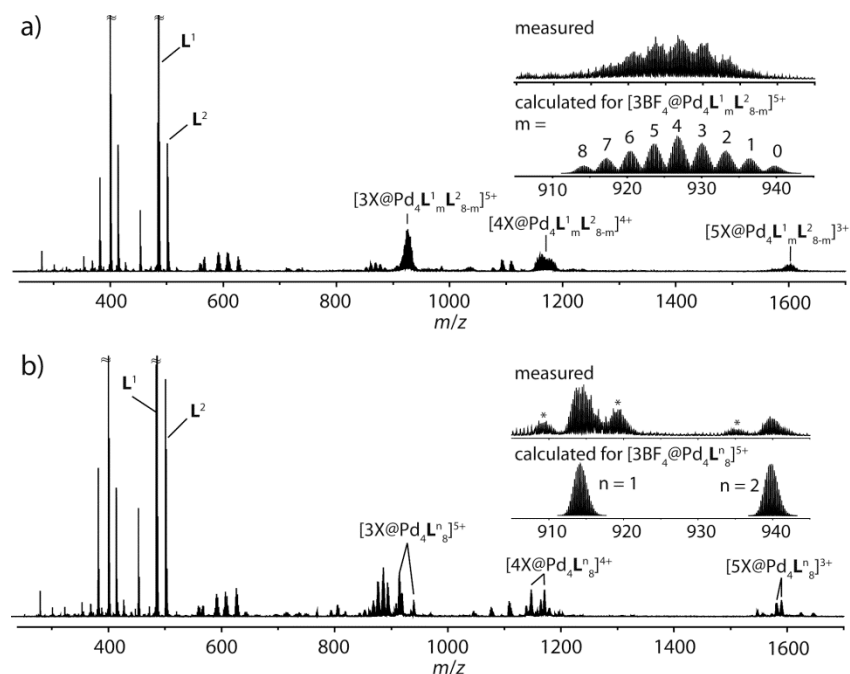


Fig. SI-4 (a) ESI-TOF mass spectra in positive mode of the solution after addition of 0.5 eq $\text{Pd}(\text{CH}_3\text{CN})_4(\text{BF}_4)_2$ to premixed ligands L^1 and L^2 (250 μL of a 2.8 mM solution for each ligand) and heating in CD_3CN at 70 $^\circ\text{C}$. The spectra shows a statistical distribution of the ligands forming the double-cages $[\text{Pd}_4\text{L}^1_m\text{L}^2_{8-m}]$ with $m = 8-0$. (b) ESI-TOF mass spectra in positive mode of the solution after mixing the double cages $[\text{Pd}_4\text{L}^1_8]$ and $[\text{Pd}_4\text{L}^2_8]$ (250 μL of a 0.35 mM solution for each cage) and heating at 70 $^\circ\text{C}$. * denotes other anion combinations with $\text{X} = \text{BF}_4^-$, F^- , NO_3^- and Cl^- .

2.1.2 Mixture of ligands L^2 and L^3 and cages $[Pd_4L^2_8]$ and $[Pd_4L^3_8]$

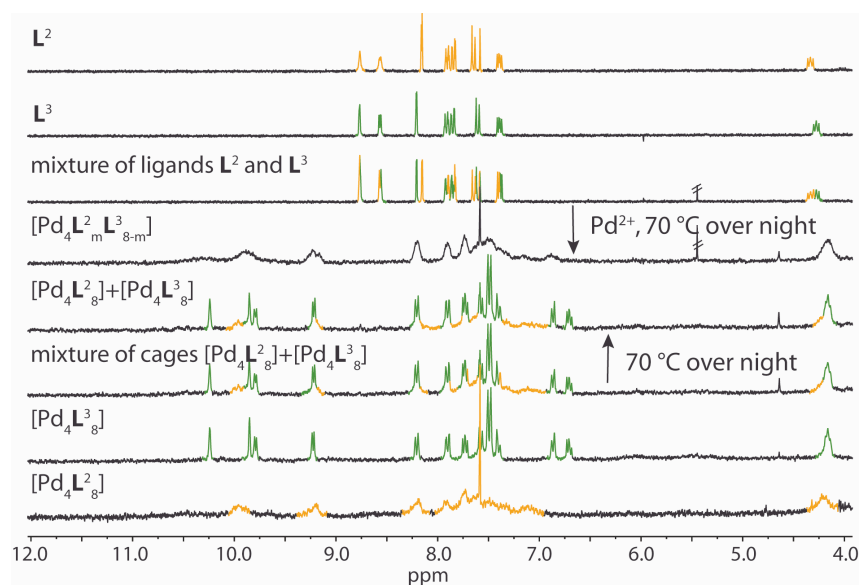


Fig. SI-5 1H NMR spectra (300 MHz, 298 K, CD_3CN) of a binary system containing two different long ligands $L^2 + L^3$ (250 μL of a 2.8 mM solution for each ligand). The outcome of the self-assembly gives mixed cages $[Pd_4L^2_mL^3_{8-m}]$, showing a statistical ligand distribution when the ligands are mixed prior to the addition of palladium and heating at 70 $^\circ C$ over night. In contrast, combining two preassembled double-cages $[Pd_4L^2_8] + [Pd_4L^3_8]$ (250 μL of a 0.35 mM solution for each cage) leads to a mixture of coexisting homogeneous structures between which ligand exchange is tremendously slowed down.

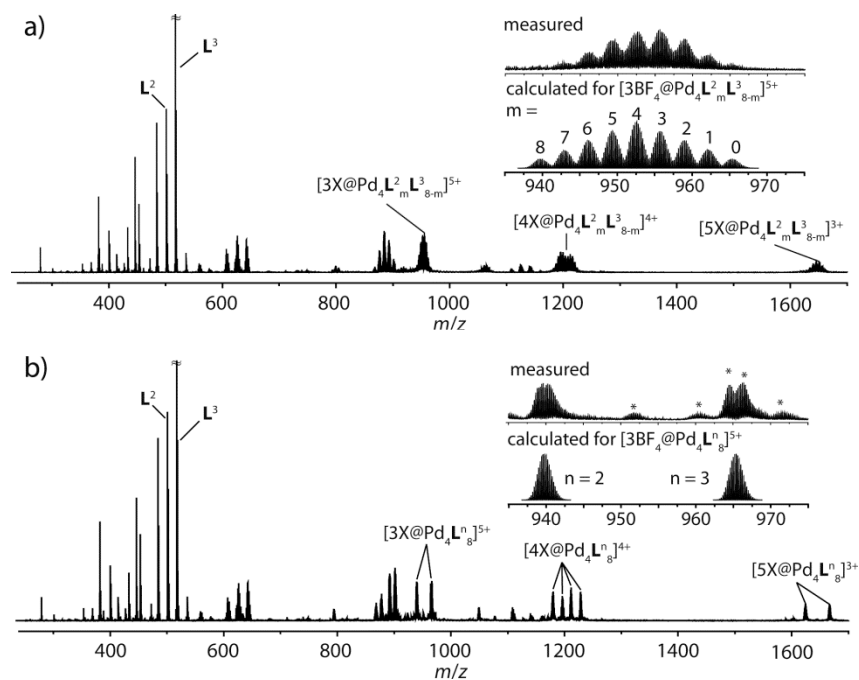


Fig. SI-6 (a) ESI-TOF mass spectra in positive mode of the solution after addition of 0.5 eq $Pd(CH_3CN)_4(BF_4)_2$ to premixed ligands L^2 and L^3 (250 μL of a 2.8 mM solution for each ligand) and heating in CD_3CN at 70 $^\circ C$. The spectra shows a statistical distribution of the ligands forming the double-cages $[Pd_4L^2_mL^3_{8-m}]$ with $m = 8-0$. (b) ESI-TOF mass spectra in positive mode of the solution after mixing the double cages $[Pd_4L^2_8]$ and $[Pd_4L^3_8]$ (250 μL of a 0.35 mM solution for each cage) and heating at 70 $^\circ C$. * denotes other anion combinations with $X = BF_4^-, F^-, NO_3^-$ and Cl^- .

2.1.3 Mixture of ligands L^2 and L^4 and cages $[Pd_4L^2_8]$ and $[Pd_2L^4_4]$

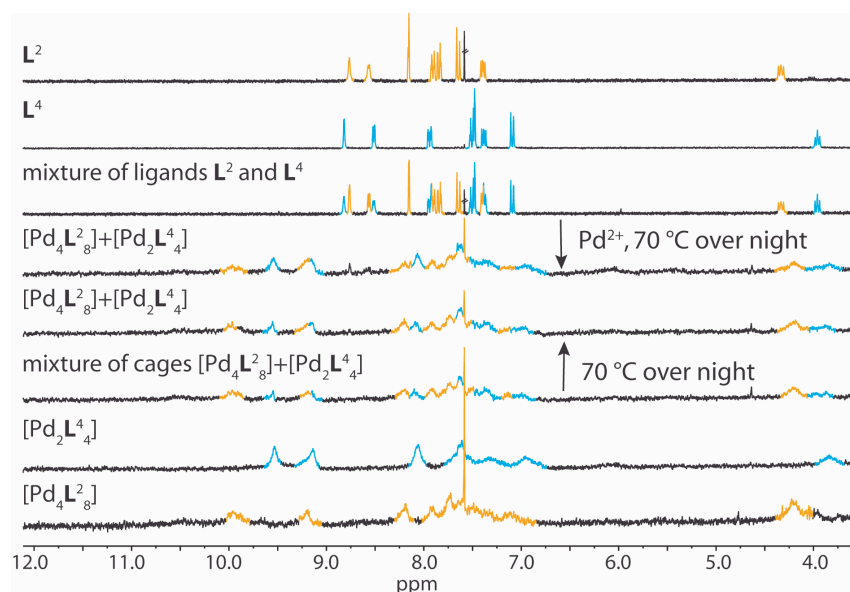


Fig. SI-7 1H NMR spectra (300 MHz, 298 K, CD_3CN) of the binary system containing the long ligand L^2 and the short ligand L^4 . The outcome of the self-assembly is independent of the order of mixing of the components. In both cases, this system shows narcissistic self-sorting behaviour to give mixture of cages $[Pd_4L^2_8]$ and $[Pd_2L^4_4]$.

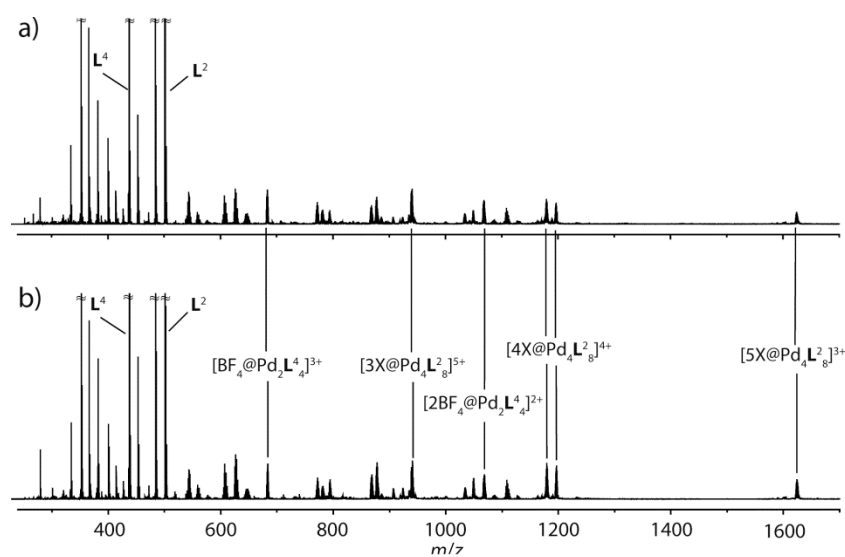


Fig. SI-8 (a) ESI-TOF mass spectra in positive mode of the solution after addition of 0.5 eq $Pd(CH_3CN)_4(BF_4)_2$ to premixed ligands L^2 and L^4 (250 μL of a 2.8 mM solution for each ligand) and heating in CD_3CN at 70 $^\circ C$. (b) ESI-TOF mass spectra in positive mode of the solution of the mixed double cages $[Pd_4L^2_8]$ and $[Pd_2L^4_4]$ (250 μL of a 0.35 mM solution for each cage) and after heating at 70 $^\circ C$. The spectra show no exchange of the ligands. $X = BF_4^-, F^-, NO_3^-$.

2.1.4 Mixture of ligands L^3 and L^4 and cages $[Pd_4L^3_8]$ and $[Pd_2L^4_4]$

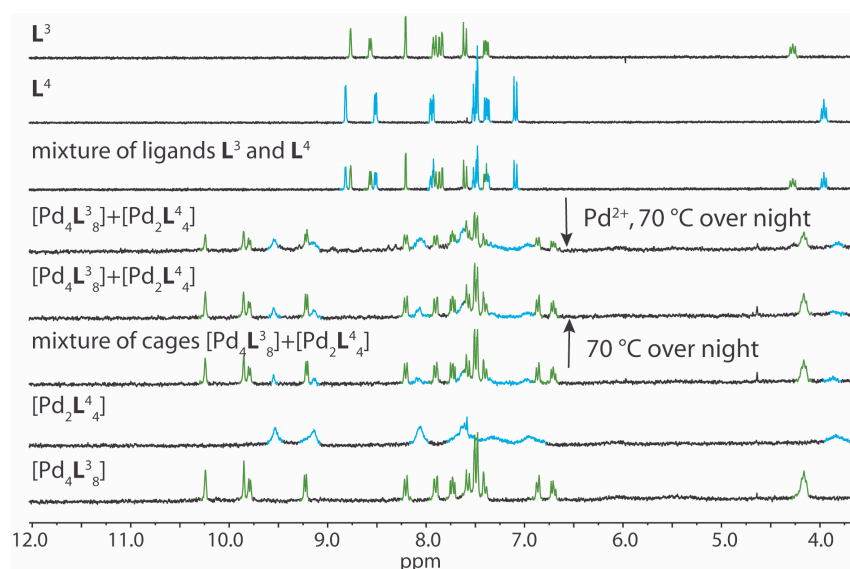


Fig. SI-9 1H NMR spectra (300 MHz, 298 K, CD_3CN) of the binary system containing the long ligand L^3 and the short ligand L^4 . The outcome of the self-assembly is independent of the order of mixing of the components. In both cases, this system shows narcissistic self-sorting behaviour to give mixture of cages $[Pd_4L^3_8]$ and $[Pd_2L^4_4]$.

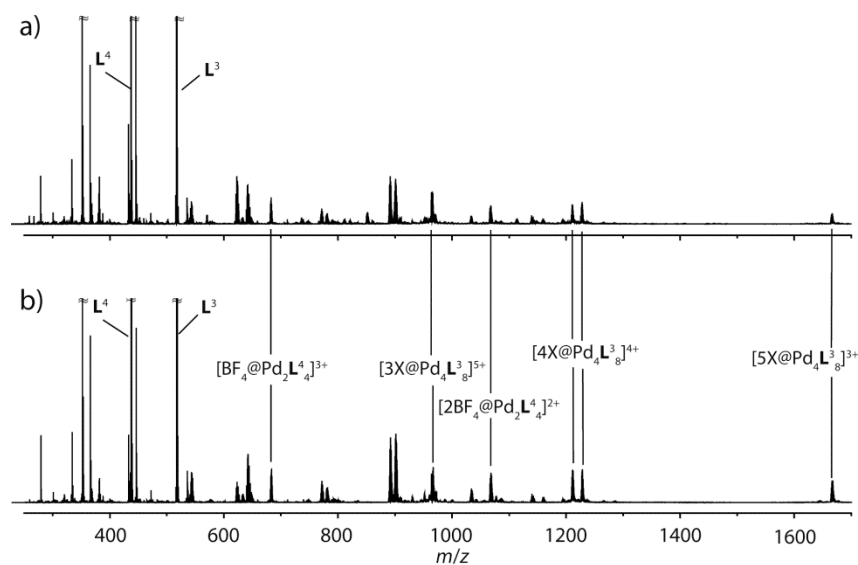


Fig. SI-10 (a) ESI-TOF mass spectra in positive mode of the solution after addition of 0.5 eq $Pd(CH_3CN)_4(BF_4)_2$ to premixed ligands L^3 and L^4 (250 μL of a 2.8 mM solution for each ligand) and heating in CD_3CN at 70 $^\circ C$. (b) ESI-TOF mass spectra in positive mode of the solution of the mixed double cages $[Pd_4L^3_8]$ and $[Pd_2L^4_4]$ (250 μL of a 0.35 mM solution for each cage) and after heating at 70 $^\circ C$. The spectra show no exchange of the ligands. $X = BF_4^-, F^-, NO_3^-$.

2.1.5 Mixture of cages $[\text{Pd}_4\text{L}^1_8]$ and $[\text{Pd}_4\text{L}^3_8]$ and 2-Picoline

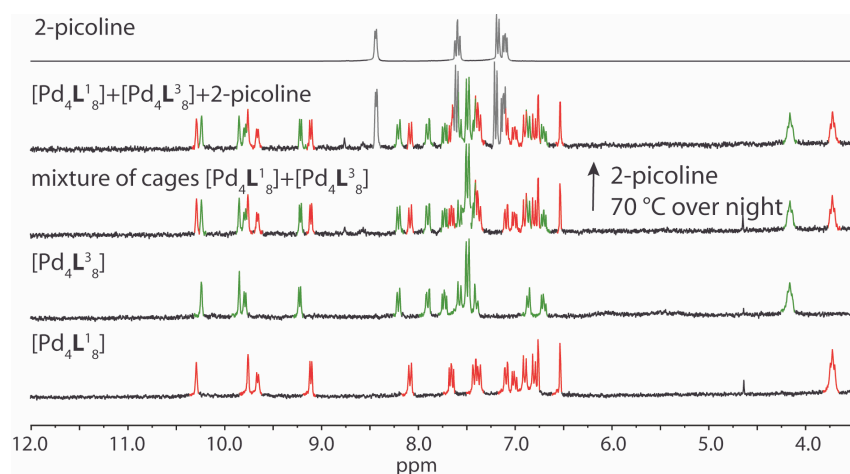


Fig. SI-11 ^1H NMR spectra (300 MHz, 298 K, CD_3CN) of the mixture of cages $[\text{Pd}_4\text{L}^1_8]$ and $[\text{Pd}_4\text{L}^3_8]$ (250 μL of a 0.35 mM solution for each cage) and 2-picoline (8 eq per cage molecule, 13 μL of a 101 mM stock solution). The outcome shows no exchange of the ligands even after heating at 70 $^\circ\text{C}$.

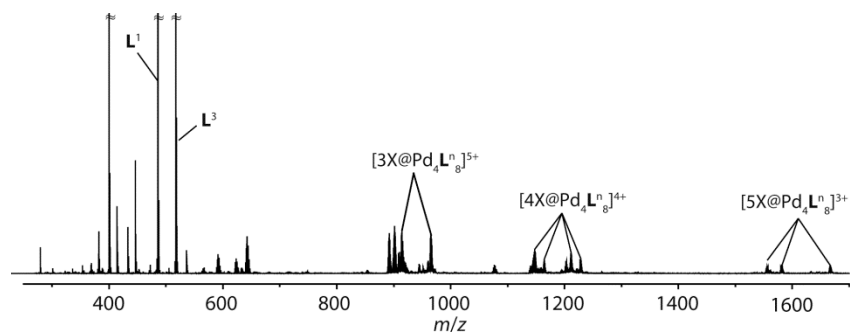


Fig. SI-12 ESI-TOF mass spectra in positive mode of the solution of the mixed double cages $[\text{Pd}_4\text{L}^1_8]$ and $[\text{Pd}_4\text{L}^3_8]$ (250 μL of a 0.35 mM solution for each cage) and 2-picoline after heating at 70 $^\circ\text{C}$. $\text{X} = \text{BF}_4^-, \text{F}^-, \text{NO}_3^-$.

2.1.6 Temporal evolution of the heated samples of the mixture of ligands L^1 and L^3 and cages $[Pd_4L^1_8]$ and $[Pd_4L^3_8]$

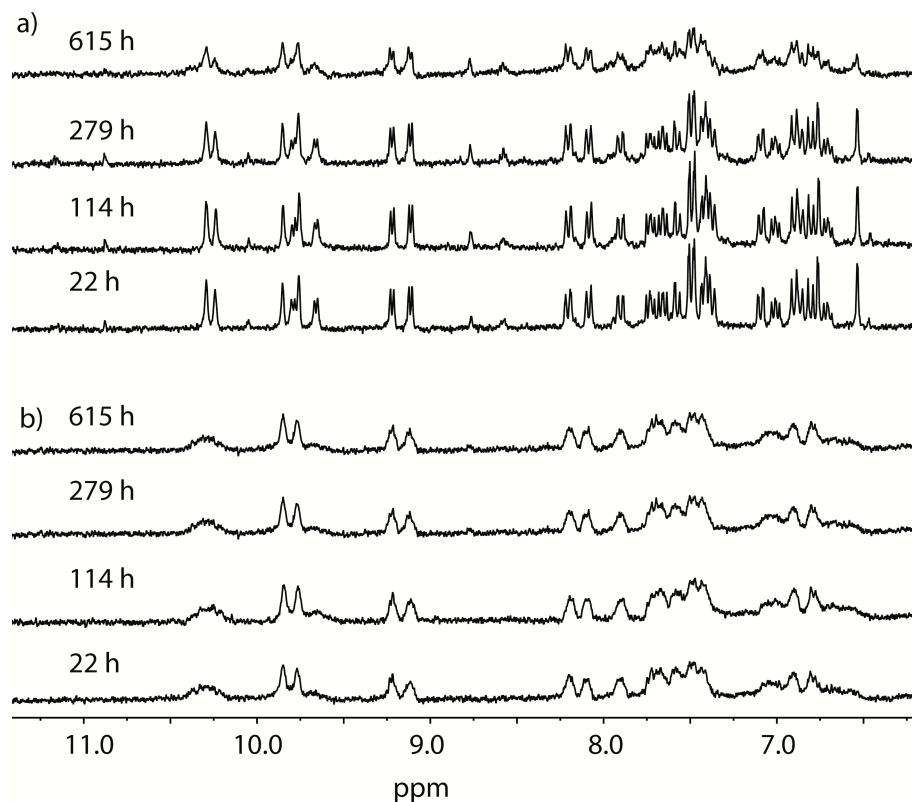


Fig. SI-13 a) 1H NMR spectra (300 MHz, 298 K, CD_3CN) of a binary system of mixed-ligand cages $[Pd_4L^1_m L^3_{8-m}]$ ($m = 1 - 8$), containing two different long ligands $L^1 + L^3$ (250 μL of a 2.8 mM solution for each ligand) after heating at 70 $^{\circ}C$ for 22 h, 114 h, 279 h and 615 h. b) In contrast, combining two preassembled double-cages $[Pd_4L^1_8] + [Pd_4L^3_8]$ (250 μL of a 0.35 mM solution for each cage) and heating at 70 $^{\circ}C$ leads to a mixture of coexisting homogeneous structures between which ligand exchange is tremendously slowed down.

¹ a) A. L. Spek, *J. Appl. Cryst.*, 2003, **36**, 7-13; b) P. van der Sluis, A. L. Spek, *Acta Cryst.*, 1990, **A46**, 194-201.

² Check-cif data:

Bond precision:	C-C = 0.0087 Å		Wavelength=0.71073
Cell:	a=21.991 (2)	b=21.991 (2)	c=31.800 (3)
	alpha=90	beta=90	gamma=90
Temperature: 100 K			
	Calculated	Reported	
Volume	15379 (3)	15379 (3)	
Space group	P 4/n n c	P 4/n n c	
Hall group	-P 4a 2bc	-P 4a 2bc	

Moiety formula	2 (C128 H108 N12 O8 Pd2 S4), 0.13 (B8 F32), 0.73 (B4 F16), 0.54 (B2 S2)	C64 H54 B1.75 Cl0.25 F7 N6 O4 Pd
Sum formula	C256 H216 B7 Cl F28 N24 O16 Pd4 S8	S2
Mr	5209.80	1302.43
Dx, g cm ⁻³	1.125	1.125
Z	2	8
Mu (mm ⁻¹)	0.363	0.363
F000	5328.0	5328.0
F000'	5324.85	
h, k, l _{max}	25, 25, 36	25, 24, 36
Nref	5936	5937
Tmin, Tmax	0.968, 0.978	0.400, 0.428
Tmin'	0.968	

Correction method= MULTI-SCAN

Data completeness= 1.000 Theta(max)= 23.837

R(reflections)= 0.0798 (4025) wR2(reflections)= 0.3031 (5937)

S = 1.060 Npar= 682

The following ALERTS were generated. Each ALERT has the format

test-name_ALERT_alert-type_alert-level.

Click on the hyperlinks for more details of the test.

🟡 Alert level B

Crystal system given = tetragonal

[THETM01_ALERT_3_B](#) The value of sine(theta_max)/wavelength is less than 0.575

Calculated sin(theta_max)/wavelength = 0.5686

[PLAT019_ALERT_1_B](#) Check _diffrn_measured_fraction_theta_full/_max 0.850

[PLAT973_ALERT_2_B](#) Large Calcd. Positive Residual Density on Pd2 1.61 eA⁻³

🟢 Alert level C

[REFNR01_ALERT_3_C](#) Ratio of reflections to parameters is < 10 for a centrosymmetric structure

sine(theta)/lambda 0.5686

Proportion of unique data used 1.0000

Ratio reflections to parameters 8.7053

[RFACR01_ALERT_3_C](#) The value of the weighted R factor is > 0.25

Weighted R factor given 0.303

[PLAT084_ALERT_3_C](#) High wR2 Value (i.e. > 0.25) 0.30

PLAT088 ALERT 3 C	Poor Data / Parameter Ratio	8.71
PLAT094 ALERT 2 C	Ratio of Maximum / Minimum Residual Density	2.19
PLAT213 ALERT 2 C	Atom F31 has ADP max/min Ratio	3.2
prolat		
PLAT220 ALERT 2 C	Large Non-Solvent C Ueq(max)/Ueq(min) ...	3.5 Ratio
PLAT222 ALERT 3 C	Large Non-Solvent H Uiso(max)/Uiso(min) ..	4.3 Ratio
PLAT342 ALERT 3 C	Low Bond Precision on C-C Bonds	0.0087 Ang.
PLAT410 ALERT 2 C	Short Intra H...H Contact H19 .. H27E ..	1.94 Ang.
PLAT905 ALERT 3 C	Negative K value in the Analysis of Variance ...	-6.187
PLAT918 ALERT 3 C	Reflection(s) # with I(obs) much smaller I(calc)	7 Check
PLAT973 ALERT 2 C	Large Calcd. Positive Residual Density on Pd1	1.48 eA-3

● Alert level G

PLAT002 ALERT 2 G	Number of Distance or Angle Restraints on AtSite	75 Note
PLAT003 ALERT 2 G	Number of Uiso or Uij Restrained non-H Atoms ...	77
PLAT042 ALERT 1 G	Calc. and Reported MoietyFormula Strings Differ	Please Check
PLAT045 ALERT 1 G	Calculated and Reported Z Differ by	0.25 Ratio
PLAT072 ALERT 2 G	SHELXL First Parameter in WGHT Unusually Large.	0.19
PLAT083 ALERT 2 G	SHELXL Second Parameter in WGHT Unusually Large.	36.09
PLAT301 ALERT 3 G	Main Residue Disorder	Percentage = 30 Note
PLAT371 ALERT 2 G	Long C(sp2)-C(sp1) Bond C4 - C6 ...	1.42 Ang.

And 3 other PLAT371 Alerts

More ...

PLAT605 ALERT 4 G	Structure Contains Solvent Accessible VOIDS of .	325 A**3
PLAT811 ALERT 5 G	No ADDSYM Analysis: Too Many Excluded Atoms	! Info
PLAT860 ALERT 3 G	Number of Least-Squares Restraints	1149 Note
PLAT869 ALERT 4 G	ALERTS Related to the use of SQUEEZE Suppressed	! Info
PLAT909 ALERT 3 G	Percentage of Observed Data at Theta(Max) still	39 %

- 0 **ALERT level A** = Most likely a serious problem - resolve or explain
3 **ALERT level B** = A potentially serious problem, consider carefully
13 **ALERT level C** = Check. Ensure it is not caused by an omission or oversight
16 **ALERT level G** = General information/check it is not something unexpected

- 3 ALERT type 1 CIF construction/syntax error, inconsistent or missing data
14 ALERT type 2 Indicator that the structure model may be wrong or deficient
12 ALERT type 3 Indicator that the structure quality may be low
2 ALERT type 4 Improvement, methodology, query or suggestion
1 ALERT type 5 Informative message, check

³ Sabrina Freye, Reent Michel, Dietmar Stalke, Martin Pawliczek, Holm Frauendorf, Guido H. Clever, *J. Am. Chem. Soc.*, 2013, **135**, 8476.